

Band Jahn-Teller Instability and Formation of Valence Bond Solid in a Mixed-Valent Spinel Oxide LiRh_2O_4

Yoshihiko Okamoto^{1,*}, Seiji Niitaka¹, Masaya Uchida¹, Takeshi Waki², Masashi Takigawa², Yoshitaka Nakatsu³, Akira Sekiyama³, Shigemasa Suga³, Ryotaro Arita^{1,†} and Hidenori Takagi^{1,4}

¹RIKEN (The Institute of Physical and Chemical Research),

Hirosawa 2-1, Wako 351-0198, Japan

²Institute for Solid State Physics,

University of Tokyo, Kashiwanoha 5-1-5,

Kashiwa 277-8581, Japan

³Division of Materials Physics,

Graduate School of Engineering Science,

Osaka University, Toyonaka 560-8531, Japan

⁴Department of Advanced Materials,

University of Tokyo, Kashiwanoha 5-1-5,

Kashiwa 277-8581, Japan

(Dated: November 1, 2018)

We have synthesized a new spinel oxide LiRh_2O_4 with a mixed-valent configuration of Rh^{3+} and Rh^{4+} . At room temperature it is a paramagnetic metal, but on cooling, a metal-insulator transition occurs and a valence bond solid state is formed below 170 K. We argue that the formation of valence bond solid is promoted by a band Jahn-Teller transition at 230 K and the resultant confinement of t_{2g} holes within the xy band. The band Jahn-Teller instability is also responsible for the observed enhanced thermoelectric power in the orbital disordered phase above 230 K.

Among the wide variety of structural categories of complex transition metal oxides, spinel, with chemical formula AB_2O_4 , is one of the most common structures and provides a unique playground for the physics of geometrical frustration. The B-sublattice of the spinel structure consists of a three-dimensional network of tetrahedra, known as the pyrochlore lattice and can underpin strong geometrical frustration effects. When antiferromagnetically coupled spins are placed on the pyrochlore lattice, long range magnetic ordering is suppressed substantially leading to, amongst other things, quantum spin liquid behavior [1]. In many cases, however, a nontrivial self-organized state of spins marginally emerges by means of coupling with lattice distortion and/or orbital ordering [2]. In analogy with spins, when a spinel B-sublattice is occupied by ions with a formally half-integer valence, suppression of charge ordering and the eventual formation of a nontrivial state of charges results. Such charge frustration has attracted much interest since the discovery of Verwey ordering in the spinel Fe_3O_4 ($\text{Fe}_1\text{Fe}_2\text{O}_4$) with 1 : 1 ratio of Fe^{2+} and Fe^{3+} on spinel B-sublattice several decades ago [3], the spatial pattern of the ordering of which has been the subject of much debate [4].

Novel mixed-valent spinels have emerged recently, notably CuIr_2S_4 [5], [6], AlV_2O_4 [7], [8] and LiV_2O_4 [9], [10]. CuIr_2S_4 and AlV_2O_4 , with nominally 1 : 1 ratio of Ir^{3+} and Ir^{4+} and V^{2+} and V^{3+} , respectively, were found commonly to show nontrivial charge ordering on cooling. In the charge ordered state, an array of spin-singlet “molecules”, Ir octamer and V heptamer, were discovered, which might be viewed as a kind of valence bond solid (VBS) [6], [8]. In LiV_2O_4 with 1 : 1 ratio of V^{3+} and

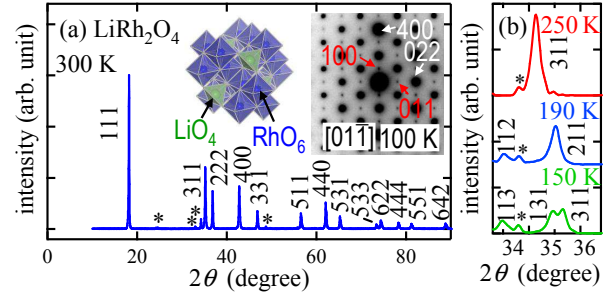


FIG. 1: (color online) Powder XRD pattern of LiRh_2O_4 at 300 K (a) and the temperature evolution of cubic 311 reflection at 250 K, 190 K and 150 K (b). The asterisks show reflections of Rh_2O_3 impurities. (a) Reflections except for those asterisked could be indexed on the basis of the cubic spinel structure with $a = 8.458 \text{ \AA}$. The inset shows the crystal structure of LiRh_2O_4 in the cubic phase, spinel structure (left), and a $[01\bar{1}]$ electron diffraction pattern at 100 K (right).

V^{4+} , no charge or spin ordering takes place down to below 1 K resulting in a novel heavy Fermion ground state being stabilised [9], [10]. This may represent a charge analogue of quantum spin liquid. LiV_2O_4 was recently discovered to show a charge ordering under pressure, where a VBS state analogous to CuIr_2S_4 and AlV_2O_4 is very likely formed [11]. The question arises whether such VBS state is common to this class of mixed-valent spinel oxides and what is the mechanism behind it.

In order to address these questions, we report the discovery and the study of a mixed-valent spinel oxide LiRh_2O_4 . LiRh_2O_4 consists of 1 : 1 ratio of low spin Rh^{3+} ($S = 0, 4d^6$) and Rh^{4+} ($S = 1/2, 4d^5$). Rh^{4+} has

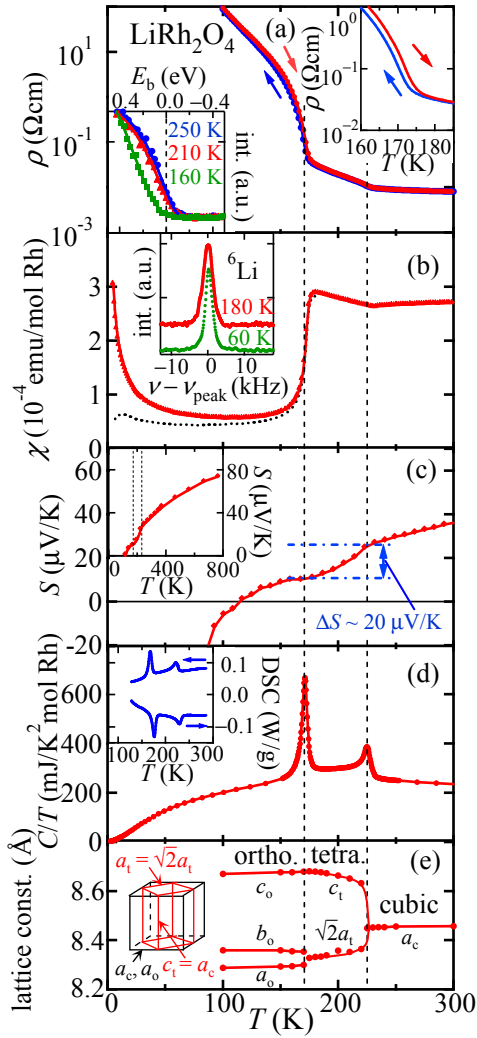


FIG. 2: (color online) Temperature dependence of resistivity (a), magnetic susceptibility (b), thermoelectric power (c), heat capacity divided by temperature (d) and the lattice constants (e) of LiRh_2O_4 polycrystalline sample. (b) The dotted line shows the susceptibility after subtracting the Curie term with a Curie constant of 1.4×10^{-3} emu/KmolRh. Inset: (a) HAXPES spectra near the Fermi level at 250 K, 210 K and 160 K (left), and the resistivity around 170 K transition (right). (b) ^6Li -NMR spectra at 180 K and 60 K. (c) Thermoelectric power up to 800 K. (d) Differential scanning calorimetry curves obtained in heating (lower) and cooling (upper) process. (e) A cubic, orthorhombic (black) and tetragonal (red) unit cell of LiRh_2O_4 .

only one hole for six-fold orbital and spin degenerate t_{2g} orbitals and the coupling with these multiple degrees of freedom may give rise to a channel to lift the degeneracy of charge distribution. We found that the ground state of this compound is a charge-ordered VBS triggered by a band Jahn-Teller transition. This strongly suggests that orbital physics drives the VBS formation. In the non-Jahn-Teller phase at high temperatures, the proximity to the Jahn-Teller instability manifests itself as a drastic

enhancement of thermoelectric power, providing us with a useful, new strategy to develop novel thermoelectric materials.

Ceramic samples of LiRh_2O_4 were synthesized by solid-state reaction. Stoichiometric amounts of Li_2O_2 and Rh_2O_3 were mixed, and the mixture was calcined at 900°C for 24 h under 5 atm. of oxygen pressure. Sample characterization and structural analysis were performed by powder X-ray diffraction (XRD) using $\text{Cu-K}\alpha$ radiation and electron diffraction. Hard X-ray photoemission spectroscopy (HAXPES) measurements with an incident photon energy of 8175 eV were performed at the beamline BL19LXU in SPring-8. ^6Li -NMR spectra were obtained by Fast Fourier Transformation of the spin-echo signals.

The powder XRD pattern of LiRh_2O_4 at room temperature in Fig. 1 (a) was consistent with the formation of a cubic spinel structure, where all the Rh sites are equivalent. Figure 2 demonstrates the temperature dependence of various physical properties of LiRh_2O_4 . The resistivity at 300 K is slightly less than 10 m Ωcm and almost temperature independent down to 230 K (Fig. 2 (a)). Since the sample is sintered polycrystal, empirically, the intrinsic resistivity can be more than one order of magnitude smaller than 10 m Ωcm , consistent with the metallic nature. In agreement with this, a well-defined Fermi cut-off was observed in the HAXPES spectrum at 250 K, as shown in the inset of Fig. 2 (a). The weakly temperature dependent paramagnetic susceptibility around 300 K can then be interpreted as Pauli paramagnetism (Fig. 2 (b)).

With decreasing temperature, we observed a kink-like anomaly both in the resistivity and in the magnetic susceptibility at 230 K, suggestive of the second order phase transition. The resistivity shows a very weak increase on cooling down to 170 K. As shown in the inset of Fig. 2 (a), the HAXPES spectrum at 210 K indicates the presence of a well-defined Fermi cut-off analogous to those at 250 K. It implies that in the temperature range between 170 K and 230 K the system remains poorly metallic and incoherent transport due to, for example, polaronic and/or disorder effects are likely responsible for the weakly semiconducting behavior of resistivity.

At 170 K, the resistivity shows a discontinuous jump of several orders of magnitude, suggestive of a metal-insulator transition, possibly associated with an ordering of charges (Fig. 2 (a)). Simultaneously, a clear shift in the Fermi edge by ~ 0.2 eV to a higher binding energy side is observed in the HAXPES spectrum (inset of Fig. 2 (a)), indicating the opening of a charge gap with an energy scale of around a fraction of eV. The presence of a tiny but clear hysteresis between warming and cooling indicates that the transition at 170 K is first order in contrast to the transition at 230 K (inset of Fig 2 (a)). Associated with the transition, the magnetic susceptibility shows discontinuous drop to a very small and almost temperature independent susceptibility, implying the formation of a spin singlet. The nonmagnetic nature

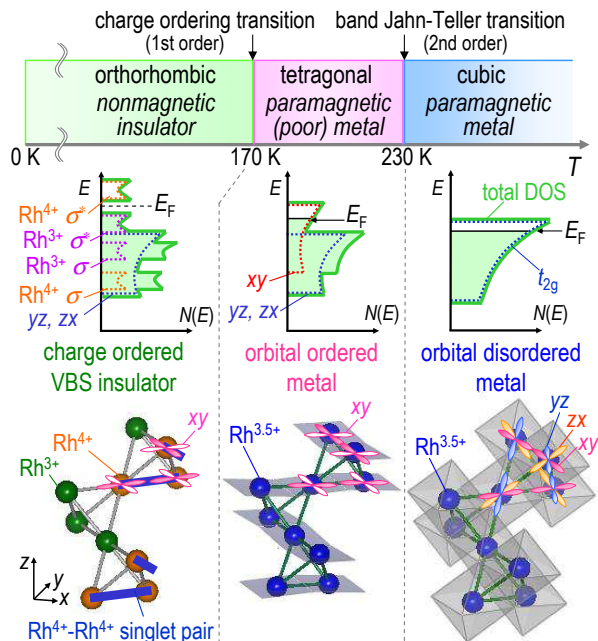


FIG. 3: (color online) Temperature variation of structural and electronic properties of LiRh_2O_4 . A proposed model for electronic structure (DOS) evolution are also shown schematically (middle), together with the real space images of corresponding orbital states (lower). In the pictures of electronic structure, thick green lines and green-colored regions show the total DOS and the occupied states of them, respectively. Dotted lines show partial DOS of individual bands.

of the insulating phase is firmly supported by ^6Li -NMR measurement shown in the inset of Fig. 2 (b): the ^6Li line width does not show any significant broadening in the insulating phase. A thermally activated decay of the spin lattice relaxation rate $1/T_1$, with a large activation energy of ~ 3000 K, was observed below 170 K, demonstrating the presence of a large spin gap [12]. This implies that very robust singlet bonds are formed in the insulating state, giving rise to the small magnetic susceptibility. Note that the energy scale of the spin gap is comparable to that of the charge gap seen in the HAXPES spectrum.

The two transitions at 230 K and 170 K are accompanied by a structural phase transition (Fig. 1 (b)). The diffraction pattern between 230 K and 170 K can be indexed with a tetragonal unit cell ($a_t = a_c/\sqrt{2} = 5.889$ Å, $c = 8.665$ Å at 200 K). Since we did not observe any extra spots in the electron diffraction compared with those in the cubic phase, the cubic-tetragonal transition can be described as a simple elongation of cubic spinel structure along [001] with space group $I4_1/amd$ (No. 141). Note that the tetragonal distortion is surprisingly large with $c/a_c = c/\sqrt{2}a_t = 1.04$ at 180 K. The pattern in the insulating state below $T_{\text{MI}} = 170$ K can be indexed with an orthorhombic cell ($a = 8.287$ Å, $b = 8.359$ Å, $c = 8.670$ Å at 100 K) [13]. In the electron diffraction patterns of the orthorhombic phase ($T < T_{\text{MI}}$), new spots including

011 and 100 clearly emerge (inset of Fig. 1), indicative of a complicated lattice distortion and the resultant lowering of symmetry with the charge ordering below $T_{\text{MI}} = 170$ K. Electron diffraction and the synchrotron XRD pattern [14] indicate that the new spots emerge at $(2l + 1, 2m, 2n)$ and $(2l, 2m + 1, 2n + 1)$, implying that the propagation vector of modulation $\mathbf{k} = (1, 0, 0)$. \mathbf{k} of LiRh_2O_4 is distinct from those of CuIr_2S_4 ($\mathbf{k} = (0, 0, 1)$, $(1/2, 1/2, 1/2)$) [6] and AlV_2O_4 ($\mathbf{k} = (1/2, 1/2, 1/2)$) [7].

The results of specific heat measurement shown in Fig. 2 (d) suggest that the transition at 230 K is in fact a drastic electronic transition in addition to the 170 K transition. The change of entropy $\Delta S_{\text{entropy}}$ associated with the transitions, estimated from specific heat and DSC measurements, was found to be 1.0 J/KmolRh at 230 K and 2.9 J/KmolRh at 170 K, which corresponds to $0.24R/\text{mole Rh}^{4+}$ and $0.70R/\text{mole Rh}^{4+}$, respectively. It may not be surprising to see a large entropy change of the order of R at 170 K transition associated with a charge ordering. It is surprising, however, to observe a large entropy change for the cubic to tetragonal transition. A structural phase transition alone, as would have been expected from the weak anomaly at 230 K in the resistivity and the magnetic susceptibility, is unlikely to be able to account for such a large entropy change. A drastic reconstruction of electronic states should be invoked to account for the hidden and large entropy change.

The 230 K transition can be naturally understood now in terms of a band Jahn-Teller transition. The large tetragonal distortion ($c/a_c \sim 1.04$) should split the triply degenerate t_{2g} band manifold into bands with stabilized yz and zx character and a band with destabilized xy character (Fig. 3). Then, while the yz and zx bands are fully occupied with 4 electrons, the xy band accommodates 0.5 holes (1.5 electrons). Stabilization of the fully occupied yz , zx bands and destabilization of the partially filled xy band enables the system to gain a Jahn-Teller energy. By inspecting the band structure of transition metal oxides with a spinel structure including LiTi_2O_4 , LiV_2O_4 and ZnRh_2O_4 , we note that the transition metal t_{2g} band commonly has relatively high density of states (DOS) near the top of the band manifold, which arises from bands with flat dispersion produced by geometrical frustration [15-18]. Recent band calculation indicated that the same is true for LiRh_2O_4 [19]. Since the Fermi level E_F should be located near the top of t_{2g} manifold in LiRh_2O_4 , a relatively high DOS at E_F can be anticipated. Such high DOS can couple with the degenerate orbital degrees of freedom, leading to a band Jahn-Teller instability. The large entropy change observed at 230 K then should be ascribed to the lifting of the band degeneracy through orbital ordering.

The high entropic state with band Jahn-Teller instability realized in the cubic phase can merit enhancing the thermoelectric power S . The presence of a flat band near E_F can drastically enhance S , as pointed out for the

well known thermoelectric Na_xCoO_2 [20] [21]. LiRh_2O_4 indeed indicates a large and positive S above 230 K, as large as $80 \mu\text{V}/\text{K}$ at 800 K, where the system remains orbitally degenerate (Fig. 2 (c)). Below the band Jahn-Teller transition at 230 K where the orbital degeneracy is lifted, S rapidly decreases by $\sim 20 \mu\text{V}/\text{K}$. Assuming that S is simply entropy per charge carrier S_{entropy}/ne , the large entropy change $\Delta S_{\text{entropy}} \sim 1.0 \text{ J}/\text{KmolRh}$ at the 230 K transition, estimated from the specific heat anomaly, gives an enhancement of thermoelectric power $\Delta S = 21 \mu\text{V}/\text{K}$ in the cubic (orbital disordered) phase, as compared with the tetragonal (orbital ordered) phase. This agrees well with the observed change of thermoelectric power $\Delta S \sim 20 \mu\text{V}/\text{K}$, implying that the large entropy change at the cubic to tetragonal transition indeed represents an “electronic” reconstruction of degenerate bands and manifests itself as an enhanced S in the cubic orbital-disordered phase.

Below 230 K, the conduction should be dominated by the carriers (0.5 holes) in the band primary with xy character. Since the xy orbitals overlap strongly along the edge of Rh-tetrahedron perpendicular to the c -axis, $[110]$ and $[\bar{1}\bar{1}0]$, the xy band should be more dispersive along these directions and quasi-one-dimensional in nature (Fig. 3). The confinement of Rh^{4+} holes within the quasi-one-dimensional xy -band, associated with the band Jahn-Teller transition, very likely promotes the formation of VBS despite the presence of charge frustration. This picture is essentially nothing but the “orbital induced Peierls” transition proposed by Khomskii and Mizokawa as a model for the VBS formation in CuIr_2S_4 [22]. CuIr_2S_4 is isoelectronic to LiRh_2O_4 but shows only one transition from a paramagnetic metal to a spin-singlet insulator [5]. The lattice distortion in the insulating phase was decomposed by Khomskii and Mizokawa into Jahn-Teller like elongation of c -axis ($c/a \sim 1.03$) and tetramer formation within the $[110]$ or $[\bar{1}\bar{1}0]$ chain and they argued that the transition is essentially a Peierls transition within the one-dimensional xy band [22]. The occurrence of a band Jahn-Teller transition in LiRh_2O_4 at higher temperature than the charge ordering transition clearly indicates that there is an intrinsic band instability in the 0.5 hole doped t_{2g} system on a frustrated pyrochlore lattice, and sets up the possibility of formation of VBS. This implies that the band Jahn-Teller instability, rather than the instability for spin-singlet bond formation, is the driving force for the suppression of charge frustration in this system. In accord with this, although the Jahn-Teller distortion presents as a common ingredient of lattice distortion in the insulating state of LiRh_2O_4 and CuIr_2S_4 , the overall lattice distortion pattern representing the charge ordering is clearly different between the two, implying the ordering pattern is determined reflecting materials-dependent details.

In conclusion, a new mixed-valent spinel oxide LiRh_2O_4 was synthesized, which provides us with an in-

triguing playground for the physics of charge-orbital-spin composites on geometrically frustrated lattices. A novel interplay of the orbital degeneracy of t_{2g} manifold and the high electronic density of states, linked to the unique geometry of the pyrochlore lattice, gives rise to a band Jahn-Teller instability in this 0.5 hole-doped system. This drives the system to a transition from an orbital-disordered metal to an orbital-ordered metal at 230 K. The large electronic entropy in the orbital disordered phase manifests itself as a remarkable enhancement of thermoelectric power, compared with the orbital-ordered metal. Materials displaying a band Jahn-Teller instability could be a good strategy to develop high performance thermoelectric materials. A charge-ordered VBS state is formed below 170 K. The formation of VBS is apparently driven by the band Jahn-Teller transition, which confines the holes within the quasi-one-dimensional xy band. Such a charge ordering induced by an orbital ordering appears to be quite ubiquitous to this class of charge frustrated mixed-valent systems.

We thank Z. Hiroi, H. Kuriyama, J. Matsuno, M. Nohara, R. S. Perry, H. Sawa, N. Shannon, A. Yamamoto, K. Kuroki, K. Held, A. V. Lukoyanov, S. Skornyakov and V. I. Anisimov for stimulating discussion, and A. Higashiya, M. Yabashi, K. Tamasaku, T. Ishikawa, S. Imada, H. Fujiwara, M. Yano, J. Yamaguchi and G. Funabashi for supporting the HAXPES measurement. A. S. acknowledges the support from the Asahi Glass Foundation. M. U. acknowledges the support by “Nanotechnology Support Project” of the Ministry of Education, Culture, Sports, Science and Technology (MEXT), Japan. This work was partly supported by a Grant-in-Aid for Scientific Research on Priority Areas “Novel States of Matter Induced by Frustration” (No. 19052008), Japan.

-
- [1] B. Canals and C. Lacroix, Phys. Rev. Lett. **80**, 2933 (1998); Phys. Rev. B **61**, 1149 (2000).
 - [2] S.-H. Lee, *et al.*, Phys. Rev. Lett. **84**, 3718 (2000); Phys. Rev. Lett. **93**, 156407 (2004); H. Tsunetsugu and Y. Motome, Phys. Rev. B **68**, 060405(R) (2003).
 - [3] E. J. W. Verwey, Nature (London) **144**, 327 (1939).
 - [4] J. P. Wright, *et al.*, Phys. Rev. Lett. **87**, 266401 (2001).
 - [5] T. Furubayashi, *et al.*, J. Phys. Soc. Jpn. **63**, 3333 (1994).
 - [6] P. G. Radaelli, *et al.*, Nature **416**, 155 (2002).
 - [7] K. Matsuno, *et al.*, J. Phys. Soc. Jpn. **70**, 1456 (2001).
 - [8] Y. Horibe, *et al.*, Phys. Rev. Lett. **96**, 086406 (2006).
 - [9] S. Kondo, *et al.*, Phys. Rev. Lett. **78**, 3729 (1997).
 - [10] C. Urano, *et al.*, Phys. Rev. Lett. **85**, 1052 (2000).
 - [11] S. Niitaka, *et al.*, *submitted*.
 - [12] T. Waki, *et al.*, *private communication*.
 - [13] Since some peaks show a noticeable broadening, there might be a further lowering of symmetry.
 - [14] H. Sawa, *et al.*, *private communication*.
 - [15] D. J. Singh, *et al.*, Phys. Rev. B **60**, 16359 (1999); Chem. Mater. **18**, 2696 (2006).
 - [16] J. Matsuno, *et al.*, Phys. Rev. B **60**, 1607 (1999).

- [17] V. I. Anisimov, *et al.*, Phys. Rev. Lett. **83**, 364 (1999).
- [18] S. Satpathy, *et al.*, Phys. Rev. B **36**, 7269 (1987).
- [19] R. Arita, *et al.*, *submitted to Phys. Rev. Lett.*
- [20] I. Terasaki, *et al.*, Phys. Rev. B **56**, R12685 (1997).
- [21] K. Kuroki and R. Arita, J. Phys. Soc. Jpn. **76**, 083707 (2007).
- [22] D. I. Khomskii and T. Mizokawa, Phys. Rev. Lett. **94**, 156402 (2005).

* Present address: Institute for Solid State Physics, Univ. of Tokyo, Kashiwanoha 5-1-5, Kashiwa 277-8581, Japan.

† Present address: Dept. of Applied Physics, Univ. of Tokyo, Hongo 7-3-1, Bunkyo-ku, Tokyo 113-8656, Japan.

Supplementary information.

Comment on the crystal structure of the charge-ordered insulating phase. Below 170 K, LiRh_2O_4 shows complicated lattice distortion due to the dimerization of Rh^{4+} . We are able to index the X-ray diffraction pattern at 100 K with an orthorhombic unit cell. Since some peaks originating from the orthorhombic phase, however, show a noticeable broadening, there might be a further lowering of symmetry. The superlattice spots including 100 and 011 in fact appears in a $[01\bar{1}]$ electron diffraction pattern. We determined a reciprocal lattice of the orthorhombic phase as shown in the supplementary figure (a), by combining it with the

electron diffraction patterns along some other directions and the synchrotron X-ray diffraction pattern. This reciprocal lattice indicates that the propagation vector of modulation is $\mathbf{k} = (1, 0, 0)$. On the other hand, Rh^{4+} - Rh^{4+} dimers are likely formed in the xy plane, because the xy band is preferentially occupied by 0.5 holes in the tetragonal phase, which is also supported by the lattice distortion and Ir^{4+} - Ir^{4+} dimerization pattern in spinel sulfide CuIr_2S_4 isoelectronic to LiRh_2O_4 . Considering that the charge ordering modulated by $\mathbf{k} = (1, 0, 0)$ and the Rh^{4+} - Rh^{4+} dimerization in the xy plane, the only two charge-ordering configuration models, shown in the supplementary figure (b), are allowed.

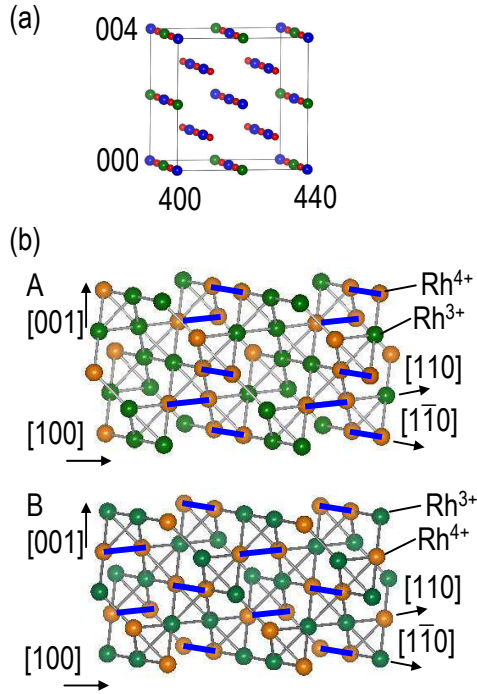


FIG. 4: Supplementary figure. (a) A schematic reciprocal lattice of the orthorhombic phase of LiRh_2O_4 determined by electron diffraction measurements (crystal axis was determined by the synchrotron X-ray powder diffraction). Blue and green spheres represent fundamental spots of the cubic spinel structure and the forbidden spots, which were observed at both 300 K of the cubic phase and at 100 K of the orthorhombic phase due to multiple reflections, respectively. Small red spheres represent new spots at $(2l + 1, 2m, 2n)$ and $(2l, 2m - 1, 2n - 1)$, where l , m and n are interger numbers, only observed at 100 K of the orthorhombic phase. (b) Pictures of two charge ordering configuration models suggested by the reciprocal lattice (a) under condition that all Rh^{4+} ions form singlet bonds within the chains, represented by thick blue lines. Both models consist of Rh tetramers with an alternation of $\text{Rh}^{4+}\text{-Rh}^{4+}\text{-Rh}^{3+}\text{-Rh}^{3+}$ along $[110]$ or $[\bar{1}\bar{1}0]$ Rh chain.